

## **Supporting Material for**

### **Organization and dynamics of Fas transmembrane domain in raft membranes and modulation by ceramide**

Bruno M. Castro, Rodrigo F.M. de Almeida, Erik Goormaghtigh, Aleksander Fedorov and Manuel Prieto

#### **Experimental design**

To understand of how lipid rafts and ceramide (Cer) modulate Fas biological function through the transmembrane domain (TMD) of Fas receptor, we have studied its membrane organization in POPC/PSM/Chol membranes with and without Cer. The TMD of Human Fas (TNFRSF6) was selected from the full sequence acquired from SwissProt database, using a hydrophobicity analysis based on the Wimley-White hydropathy scale, performed with Membrane Protein Explorer (MPEx) software (1). The recovered sequence had 19 residues, ranging from Leu<sup>174</sup> to Arg<sup>192</sup>. Ser<sup>172</sup> and Asn<sup>173</sup> were added to that sequence, since interfacial polar residues directly intervene in the orientation of transmembrane segments, helping proteins to adopt their proper conformation in the membrane (2). The final sequence for Fas TMD was n-Ser-Asn-Leu-Gly-Trp-Leu-Cys-Leu-Leu-Leu-Leu-Pro-Ile-Pro-Leu-Ileu-Val-Trp-Val-Lys-Arg-C. The POPC/PSM/Chol system was chosen because it is a fully characterized “model raft system” (3,4), that displays fluid-fluid phase separation as it is proposed to occur in the plasma membrane of cells (5,6). The compositions of the lipid mixtures studied are contained within the tie-line that spans the liquid-disordered (ld)/liquid-ordered (lo) phase coexistence region of the POPC/PSM/Chol phase diagram, enclosing the “canonical raft mixture” (1:1:1) (Fig. S1) (3). The mixtures that define this tie-line have been extensively studied in terms of phase properties and domain size (3,4). Moreover, Cer effects on those membrane properties have also been determined and quantified (7). When

performing studies along a tie-line, the lever rule applies, meaning that the fraction of each phase is changing but its composition is constant and given by the extremes of the tie-line (8). In these conditions, we ensure that the changes observed in Fas TMD properties do not arise from any alterations in the lipid composition of each phase, and can be quantitatively related to the amount of each phase.

### **Infrared Spectroscopy**

Attenuated total reflection infrared (ATR-FTIR) spectra were recorded in the double-sided, forward-backward mode on a Bruker IFS55 FTIR spectrophotometer (Ettlingen, Germany) equipped with a liquid nitrogen cooled mercury cadmium telluride (MCT) detector at a resolution of  $2\text{ cm}^{-1}$  and with an aperture of 3.5 mm. The spectrometer was placed on vibration-absorbing sorbothane mounts (Edmund Industrial Optics, Barrington, NJ) and it was continuously purged with dry air (Whatman 75-62, Haverhill, MA). For a better stability, the purging of the spectrometer optic compartment (5 L/min) and the sample compartment (10–20 L/min) were dissociated and controlled independently by flowmeters (Fisher Bioblock Scientific, Illkirch, France). The internal reflection element was a germanium ATR plate (52×20×2mm, ACM, Villiers St. Frédéric, France) with an aperture angle of  $45^\circ$  yielding 25 internal reflections. 128 accumulations were performed to improve the signal/noise ratio. For polarization experiments, a Perkin-Elmer gold wire grid polarizer was positioned before both the sample and the reference plate.

The germanium crystals were washed in Superdecontamine (Intersciences, AS, Brussels, Belgium), rinsed with distilled water, methanol and chloroform, and finally placed for 2 min in a plasma cleaner PDC23G (Harrick, Ossining, NY) working under reduced air pressure. Measurements were carried out at  $22^\circ\text{C}$ .

*Sample preparation.* Oriented multilayers were formed by slow evaporation of 100  $\mu\text{L}$  of the sample on one side of the ATR plate, yielding a semi-dry film bearing residual water molecules (9,10). The ATR plate was then sealed in a universal sample holder (Specac, Orpington, UK). A computer controlled elevator (WOW Company SA, Belgium) allowed the different lanes to be analysed separately so that baseline and sample could be recorded on the same crystal with the same polarisation. Films contained 10  $\mu\text{g}$  of peptide for all the experiments.

### **Fluorescence quenching experiments**

The accessibility to the aqueous solvent of Fas TMD in ld and lo-rich ( $X_{\text{lo}} = 0.86$ ) liposomes was studied by monitoring the fluorescence quenching of Fas Trp induced by increasing amounts of acrylamide added from a 3 M stock solution. Trp fluorescence intensity ( $\lambda_{\text{exc}} = 295$  nm with  $\lambda_{\text{em}} = 340$  nm) was corrected for sample dilution and inner filter effects according to (11). Data was analyzed according to the Stern-Volmer relationship:

$$\frac{I_0}{I} = 1 + K_{SV}[Q] \quad (\text{S1})$$

where  $I_0$  and  $I$  are the steady-state fluorescence intensities in the absence and in the presence of quencher, respectively, and  $[Q]$  is the quencher concentration. Because no significant deviation was detected in these plots (Fig. S2), the static quenching contribution was considered to account for less than 10% of the measured signal, and the Stern-Volmer constant,  $K_{SV}$ , was directly obtained from the slope of the linear relationship (12). This parameter represents the weighted sum of the individual constants of the emitting Trp residues and was used to calculate the bimolecular rate constant of the quenching process,  $k_Q$ , from the following expression:

$$K_{SV} = k_Q \langle \tau \rangle_0 \quad (\text{S2})$$

where

$$\langle \tau \rangle_0 = \frac{\sum_i \alpha_i \tau_i^2}{\sum_i \alpha_i \tau_i} \quad (\text{S3})$$

is the mean fluorescence lifetime in the absence of quencher. This parameter was determined experimentally and was found to be respectively, 5.19 ns and 2.78 ns, for Fas TMD Trp in ld and lo-rich membranes.

The Stern-Volmer plots for Fas TMD Trp fluorescence quenching by acrylamide in ld and lo-rich membranes determined according to Eq. S1 are presented in Fig. S2. The  $K_{SV}$  values extracted from the slopes of Fig. S2 were  $1.99 \text{ M}^{-1}$  and  $3.43 \text{ M}^{-1}$  for ld and lo-rich membranes, respectively. These were used to calculate the bimolecular rate constant of the quenching process,  $k_Q$ , according to Eq. S2, using the mean fluorescence lifetimes in the absence of quencher (see above). The values of  $k_Q = 1.24 \times 10^9 \text{ M}^{-1} \text{ s}^{-1}$  for lo-rich and  $k_Q = 3.83 \times 10^8 \text{ M}^{-1} \text{ s}^{-1}$  for ld liposomes show that the accessibility of acrylamide to Fas TMD Trp is higher in the lo than in the ld phase.

*Sample preparation.* MLVs containing the appropriate amounts of lipid and peptide (1.0 mM total lipid with 0.35 mol % total lipid of TMD CD95) were prepared as described in the Material section of the manuscript. From these, LUVs were prepared by the extrusion technique as described previously (7) and an appropriate volume of these suspensions was used in the quenching assays.

### **Fas TMD effects in the membrane properties of POPC/PSM/Chol mixtures.**

*Lipid phase boundaries of the POPC/PSM/Chol phase diagram.* To evaluate the eventual perturbation induced by Fas TMD on the phase boundaries of the POPC/PSM/Chol phase diagram, *trans*-parinaric acid (t-PnA) lifetimes were measured in the absence and presence of

the peptide as previously described (13) (Fig. S2A). Briefly, t-PnA (obtained from Molecular Probes, Leiden, The Netherlands) in an ethanol stock solution was added to POPC/PSM/Chol MLVs with and without Fas TMD at a probe:lipid ratio of 1:500 (the final ethanol volume was always less than 0.5%, to prevent bilayer destabilization (14)). The samples were equilibrated by freeze-thaw cycles and subsequently kept overnight at room temperature. t-PnA injection procedure allowed the use of the same sample for Fas photophysical measurements and subsequently the t-PnA fluorescence decays studies. t-PnA emission was measured at  $\lambda_{em}=405\text{nm}$  using the magic angle ( $54.7^\circ$ ) relative to the vertically polarized excitation beam ( $\lambda_{ex}=320\text{nm}$ ) produced by a frequency doubled Rhodamine 6G laser (3), and its fluorescence lifetimes were determined as previously described (15).

From Fig. S2A it is clear that t-PnA mean fluorescence lifetimes are not affected by the presence of Fas TMD and are similar to t-PnA mean fluorescence lifetimes described in the literature for this ternary mixture (7). These results show that the lipid phase boundaries of the POPC/PSM/Chol phase diagram are not affected by Fas peptide.

*Lipid domain sizes in POPC/PSM/Chol mixtures.* To assess possible effects of the peptide on the size of the lipid domains formed in the POPC/PSM/Chol mixtures, a Förster resonance energy transfer (FRET) experiment was performed (Fig. S2B). The FRET efficiency ( $E$ ) between a donor and acceptor that are preferentially located in different lipid phases can be used to estimate the sizes of lipid domains in the nanometer scale (4,7). These experiments were carried out in LUVs (1mM total lipid concentration) as previously described (7). The vesicles contained 1,2-dipalmitoyl-*sn*-glycero-3-phosphoethanolamine-N-(7-nitro-2-1,3-benzoxa-diazol-4-yl) (NBD-DPPE) (Molecular Probes, Leiden, The Netherlands) and 1,2-dioleoyl-*sn*-glycero-3-phosphoethanolamine-N-(lissamine rhodamine B sulfonyl) (Rh-DOPE) (Avanti Polar Lipids, Alabaster, AL) as the donor/acceptor pair for FRET between

the lo and ld phases at a probe/lipid (P/L) ratio of 1:1000 and 1:200, respectively. For this donor P/L ratio, no donor self-quenching or energy homotransfer takes place (16). Data analysis was performed using the FRET model described in detail by de Almeida *et al.* (4). For a random distribution of NBD-DPPE and Rho-DOPE, both in-plane (cis) and out-of-plane (trans) energy transfer occur. For the in-plane FRET, the decay of the donor fluorescence in the presence of acceptor, assuming a radius of exclusion of acceptors ( $R_e$ ) around the donor is:

$$\rho_{cis}(t) = \exp\left\{-\pi R_0^6 n \gamma \left[\frac{2}{3}, \left(\frac{R_0}{R_e}\right)^6 (t/\bar{\tau})^{1/3} + \pi R_e^2 n \left(1 - \exp\left[-\left(\frac{R_0}{R_e}\right)^6 (t/\bar{\tau})\right]\right)\right]\right\} \quad (S4)$$

where  $n$  is the surface density of acceptors,  $R_0$  is the Förster radius and

$$\gamma(x, y) = \int_0^y z^{x-1} \exp(-z) dz \quad (S5)$$

is the incomplete Gamma function.

Energy transfer to acceptors in the opposing membrane leaflet results in a donor decay described by:

$$\rho_{cis}(t) = \exp\left\{-\frac{2c}{\Gamma(2/3)b} \int_0^{w/\sqrt{w^2+R_e}} [1 - \exp(-tb^3 \alpha^6)] \alpha^{-3} d\alpha\right\} \quad (S6)$$

where

$$c = \Gamma(2/3) n \pi R_0^2 \bar{\tau}^{-1/3} \quad (S7)$$

In this equation,  $\Gamma$  is the complete Gamma function,  $b = \left(R_0/w\right)^2$ , and  $w$  is the interplanar donor-acceptor distance. This value was fixed as  $w = 40\text{\AA}$  for ld phase and  $w = 49\text{\AA}$  for the lo phase (4). In the calculation of the surface density of acceptors, an area per molecule of  $66.4\text{\AA}^2$  for POPC (17),  $47.8\text{\AA}^2$  for PSM (18), and  $37.7\text{\AA}^2$  for Chol (19) were considered. The condensation effect of Chol was taken into account (19).

The donor decay in the presence of acceptor is given by:

$$i_{DA}(t) = i_D(t)\rho_{cis}(t)\rho_{trans}(t) \quad (S8)$$

The FRET efficiency is computed numerically through the relation  $E = 1 - (\bar{\tau}_{DA}/\bar{\tau}_D)$ .

NBD-DPPE emission was measured at  $\lambda=536\text{nm}$  with excitation at  $\lambda=428\text{nm}$  produced by a frequency doubled Ti-Sa laser (4) and its fluorescence lifetimes were determined as described previously (7).

The FRET efficiencies ( $E$ ) obtained for membranes with Fas-TMD (Fig. S2B) are lower as compared to  $E$  measured in membranes without peptide, showing that the lipid domains become larger in the presence of Fas-TMD. Possibly the peptide modulates the line tension at the domains interface. In addition, taking into account all the photophysical results, another contribution to the decrease of  $E$  at high  $X_{lo}$ , might come from the organization of Fas-TMD in the lo phase. In this phase, if Fas-TMD settles embedded near the interfacial region of the lipid bilayer, adopting a conformation that pushes the lipids apart laterally (although favoring the interactions between bilayers, due to the observed aggregation), this would result in an increase of the surface area of the membrane. Thus, the surface density of acceptors would decrease, leading to a decrease in  $E$ .

### **Fas TMD diffusion coefficient obtained from a dynamic self-quenching process**

In pure ld membranes, Fas TMD Trp quantum yield-weighted lifetimes decrease for the highest concentration studied (3.0 mol% total lipid) (Fig. 2). This can be interpreted as a result of a dynamic self-quenching process. The effect of collisional self-quenching on the fluorescence lifetime of a molecule with a complex decay is described by the modified Stern-Volmer equation (20):

$$\frac{\bar{\tau}_0}{\bar{\tau}_q} = 1 + k_q \times \langle \tau \rangle_{0q} \times [F] \quad (S9)$$

where  $\langle \tau \rangle_{0q}$  is given by

$$\langle \tau \rangle_{0q} = \frac{\sum_i \alpha_{0i} \tau_i \tau_{0i}}{\sum_i \alpha_{0i} \tau_i} \quad (\text{S10})$$

The subscript 0 indicates the absence of quencher (in our case, the values for the sample with lowest peptide concentration),  $k_q$  is the bimolecular quenching rate constant and  $[F]$  is the concentration of fluorophore. The bimolecular rate constant is related to the diffusion coefficient of the fluorophore ( $D$ ) via the Smoluchowski equation taking into account transient effects (21),

$$k_q = 4\pi N_A (2R_c)(2D) \left[ 1 + 2R_c / (2\bar{\tau}_{0q} D) \right]^{1/2} \quad (\text{S11})$$

where  $N_A$  is the Avogadro number and  $R_c$  the collisional radius.

This equation assumes that diffusion occurs in an isotropic three-dimensional medium (22).

The quantum yield-weighted lifetime of the more diluted sample of Fas TMD (0.35 mol%) is considered the limiting  $\bar{\tau}_0$ . From Eq. S9, a value of  $k_q = 2.1 \times 10^{-8} \text{ mol}^{-1} \text{ dm}^3 \text{ s}^{-1}$  is obtained for 3.0 mol% of Fas TMD in a pure ld membrane. This value assumes a random distribution of peptide analytical concentration in the lipid  $[F] = 0.041\text{M}$ , determined on the basis of its 3.0 mol% concentration and considering the mole fraction of POPC, PSM and Chol in the lipid mixture and their volumes of  $1256.5 \text{ \AA}^3$ ,  $1165.2 \text{ \AA}^3$  and  $624.8 \text{ \AA}^3$ , respectively (23). The diffusion coefficient of Fas TMD peptide is obtained from Eq. 7, assuming a collisional radius for Fas TMD of  $10 \text{ \AA}$ . The obtained value of  $D = 11 \times 10^{-9} \text{ cm}^2 \text{ s}^{-1}$  is in the same order of magnitude of those typically found for TMD proteins diffusion in an ld phase ( $D = 10\text{-}70 \times 10^{-9} \text{ cm}^2 \text{ s}^{-1}$  (13,24,25)), showing that the approximations used in the diffusive model employed are valid.

## References

1. Snider,C., S.Jayasinghe, K.Hristova, and S.H.White. 2009. MPEX: A tool for exploring membrane proteins. *Protein Sci.* 18:2624-2628.
2. Holt,A. and J.A.Killian. 2010. Orientation and dynamics of transmembrane peptides: the power of simple models. *Eur. Biophys. J. Biophys. Lett.* 39:609-621.
3. de Almeida,R.F.M., A.Fedorov, and M.Prieto. 2003. Sphingomyelin/phosphatidylcholine/cholesterol phase diagram: Boundaries and composition of lipid rafts. *Biophys. J.* 85:2406-2416.
4. de Almeida,R.F.M., L.M.S.Loura, A.Fedorov, and M.Prieto. 2005. Lipid rafts have different sizes depending on membrane composition: A time-resolved fluorescence resonance energy transfer study. *J. Mol. Biol.* 346:1109-1120.
5. London,E. and D.A.Brown. 2000. Insolubility of lipids in Triton X-100: physical origin and relationship to sphingolipid/cholesterol membrane domains (rafts). *Biochim. Biophys. Acta-Biomembr.* 1508:182-195.
6. Stöckl,M., A.P.Plazzo, T.Korte, and A.Herrmann. 2008. Detection of lipid domains in model and cell membranes by fluorescence lifetime imaging microscopy of fluorescent lipid analogues. *J. Biol. Chem.* 283:30828-30837.
7. Silva,L.C., R.F.M.de Almeida, B.M.Castro, A.Fedorov, and M.Prieto. 2007. Ceramide-domain formation and collapse in lipid rafts: Membrane reorganization by an apoptotic lipid. *Biophys. J.* 92:502-516.
8. Rhines,F.N. 1956. Phase Diagrams in Metallurgy: Their Development and Application. McGraw-Hill, New York, NY.

9. Goormaghtigh,E., V.Cabiaux, and J.M.Ruyschaert. 1990. Secondary structure and dosage of soluble and membrane proteins by attenuated total reflection Fourier-transform infrared spectroscopy on hydrated films. *Eur. J. Biochem.* 193:409-420.
10. Goormaghtigh,E., V.Raussens, and J.M.Ruyschaert. 1999. Attenuated total reflection infrared spectroscopy of proteins and lipids in biological membranes. *Biochim. Biophys. Acta-Rev. Biomembr.* 1422:105-185.
11. Coutinho,A. and M.Prieto. 1993. Ribonuclease T1 and alcohol dehydrogenase fluorescence quenching by acrylamide: A laboratory experiment for undergraduate students. *J. Chem. Edu.* 70:425-428.
12. Eftink,M.R. 1991. Fluorescence Techniques for Studying Protein-Structure. *Methods Biochem. Anal.* 35:127-205.
13. de Almeida,R.F.M., L.M.S.Loura, M.Prieto, A.Watts, A.Fedorov, and F.J.Barrantes. 2004. Cholesterol modulates the organization of the gamma M4 transmembrane domain of the muscle nicotinic acetylcholine receptor. *Biophys. J.* 86:2261-2272.
14. Vierl,U., L.Lobbecke, N.Nagel, and G.Cevc. 1994. Solute effects on the colloidal and phase-behavior of lipid bilayer-membranes - Ethanol-Dipalmitoylphosphatidylcholine mixtures. *Biophys. J.* 67:1067-1079.
15. de Almeida,R.F.M., L.M.S.Loura, A.Fedorov, and M.Prieto. 2002. Nonequilibrium phenomena in the phase separation of a two-component lipid bilayer. *Biophys. J.* 82:823-834.

16. Loura,L.M.S., A.Fedorov, and M.Prieto. 2001. Fluid-fluid membrane microheterogeneity: A fluorescence resonance energy transfer study. *Biophys. J.* 80:776-788.
17. Chiu,S.W., E.Jakobsson, S.Subramaniam, and H.L.Scott. 1999. Combined Monte Carlo and molecular dynamics simulation of fully hydrated dioleoyl and palmitoyloleoyl phosphatidylcholine lipid bilayers. *Biophys. J.* 77:2462-2469.
18. Li,X.M., J.M.Smaby, M.M.Momsen, H.L.Brockman, and R.E.Brown. 2000. Sphingomyelin interfacial behavior: The impact of changing acyl chain composition. *Biophys. J.* 78:1921-1931.
19. Smaby,J.M., M.M.Momsen, H.L.Brockman, and R.E.Brown. 1997. Phosphatidylcholine acyl unsaturation modulates the decrease in interfacial elasticity induced by cholesterol. *Biophys. J.* 73:1492-1505.
20. Sillen,A. and Y.Engelborghs. 1998. The correct use of "average" fluorescence parameters. *Photochem. Photobiol.* 67:475-486.
21. Umberger,J.Q. and V.K.Lamer. 1945. The kinetics of diffusion controlled molecular and ionic reactions in solution as determined by measurements of the quenching of fluorescence. *J. Am. Chem. Soc.* 67:1099-1109.
22. Owen,C.S. 1975. 2-Dimensional Diffusion-Theory - Cylindrical Diffusion-Model Applied to Fluorescence Quenching. *Journal of Chemical Physics* 62:3204-3207.
23. Greenwood,A.I., S.Tristram-Nagle, and J.F.Nagle. 2006. Partial molecular volumes of lipids and cholesterol. *Chem. Phys. Lipids* 143:1-10.

24. Ramadurai,S., A.Holt, V.Krasnikov, G.van den Bogaart, J.A.Killian, and B.Poolman. 2009. Lateral diffusion of membrane proteins. *J. Am. Chem. Soc.* 131:12650-12656.
25. Ramadurai,S., A.Holt, L.V.Schafer, V.V.Krasnikov, D.T.S.Rijkers, S.J.Marrink, J.A.Killian, and B.Poolman. 2010. Influence of hydrophobic mismatch and amino acid composition on the lateral diffusion of transmembrane peptides. *Biophys. J.* 99:1447-1454.

**Fig. S1** – POPC/PSM/Chol ternary phase diagram. The ternary mixtures used in this study are represented as open circles. The tie-line that contains these mixtures is also presented (solid line connecting each circle). ld, lo, and g are the liquid-disordered, liquid-ordered, and gel phases, respectively. See de Almeida *et al.* (3) for further details.

**Fig. S2** – Stern-Volmer plots for acrylamide quenching of Fas TMD (0.35 mol% total lipid) Trp fluorescence in ld (open symbols) and lo-rich ( $X_{lo} = 0.86$ ) (solid symbols) POPC/PSM/Chol membranes (1.0 mM total lipid). The solid line is the linear fit of Eq. S1 to the data with  $K_{SV}$  of  $1.99 \text{ M}^{-1}$  ( $R^2 = 0.975$ ) and  $3.43 \text{ M}^{-1}$  ( $R^2 = 0.978$ ) for ld and lo-rich membranes, respectively.

**Fig. S3** – The effect of Fas TMD on the boundaries and domain size of the POPC/PSM/Chol phase diagram. (A) t-PnA mean fluorescence lifetime ( $\langle \tau \rangle$ ) as a function of  $X_{lo}$  in the absence (black circles) and presence (white circles) of 0.35 mol% peptide at room temperature. (B) Variation of FRET efficiency,  $E$ , for the donor/acceptor pair NBD-DPPE/Rho-DOPE as a function  $X_{lo}$  in the absence (black circles) and presence (white circles) of 0.35 mol% peptide. Experimental data are represented by circles symbols, and square symbols are the values calculated for a random distribution of donors and acceptors (see text above) and present a good agreement with the experimental values measured for membranes without Fas.

Figure S1

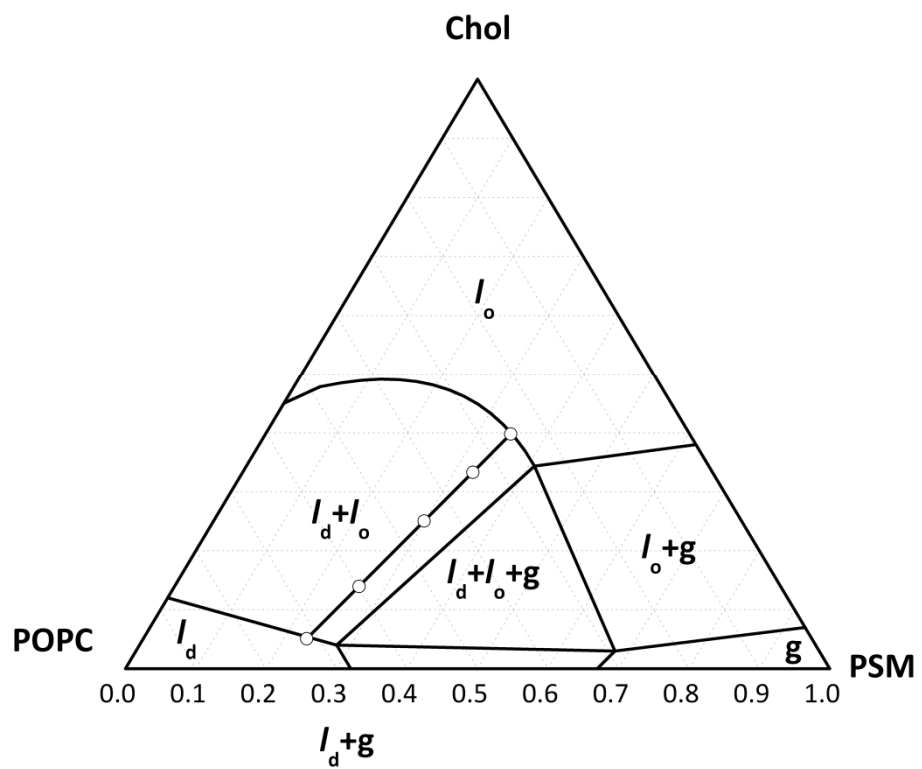


Figure S2

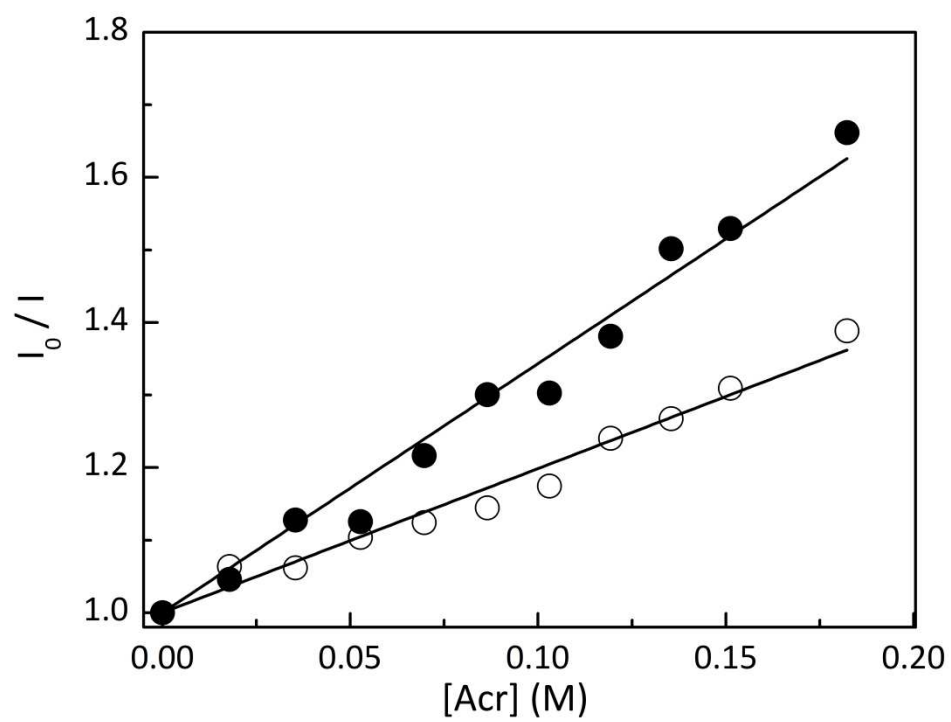
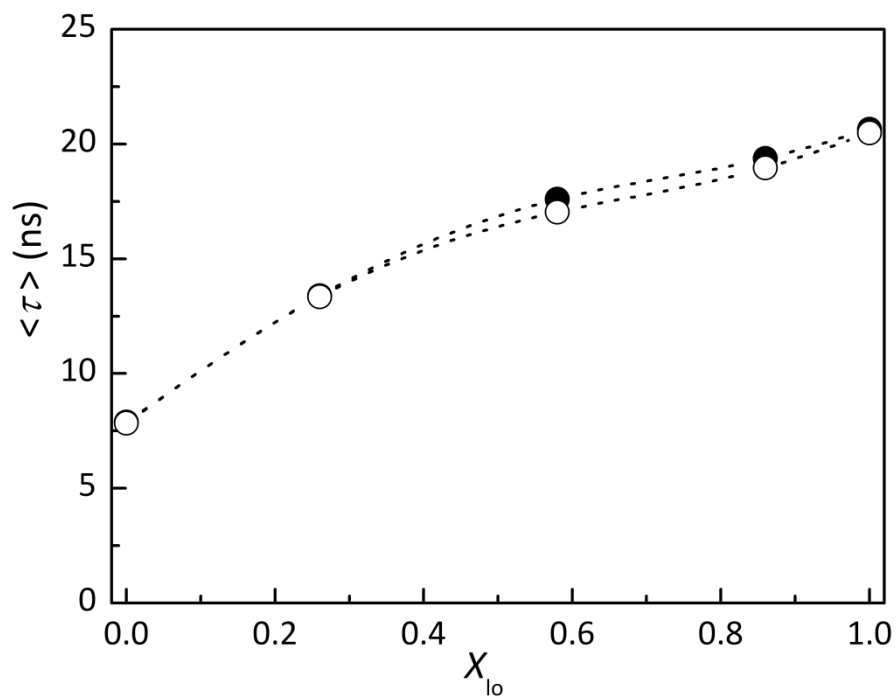


Figure S3

A



B

